Nanoscale

ROYAL SOCIETY OF CHEMISTRY

PAPER

View Article Online
View Journal | View Issue

Check for updates

Cite this: *Nanoscale*, 2022, **14**, 15060

Graphene performs the role of an electron donor in covalently interfaced porphyrin-boron azadipyrromethene dyads and manages photoinduced charge-transfer processes†

Ruben Canton-Vitoria,‡[a] Ajyal Z. Alsaleh,‡[a] Georgios Rotas,[a,d] Yusuke Nakanishi,[c,e] Hisanori Shinohara,[c] Francis D' Souza *[b] and Nikos Tagmatarchis *[a]

Herein, we introduced the versatility of free-base and zinc-metallated porphyrin (H_2P and ZnP, respectively) to combine with boron azadipyrromethene (azaBDP) NIR absorbing species, for extending their photophysical interest and covalently anchored onto graphene. In particular, the covalent functionalization of graphene with those H_2P-azaBDP and ZnP-azaBDP dyads ensured an invariable structure, in which both chromophores and graphene are in intimate contact, free of aggregations and impurities. Both H_2P-azaBDP and ZnP-azaBDP dyads were found to perform energy transfer processes between the chromophores, however, only ZnP-azaBDP confirmed additional charge separation between the chromophores yielding the $ZnP^{\bullet+}$-$azaBDP^{\bullet-}$ charge-separated state. On the other hand, graphene in (H_2P-azaBDP)-graphene and (ZnP-azaBDP)-graphene hybrids was found to act as an electron donor, yielding (H_2P-$azaBDP^{\bullet-}$)-$graphene^{\bullet+}$ and (ZnP-$azaBDP^{\bullet-}$)-$graphene^{\bullet+}$ charge-separated states at an ultrafast timescale. The creation of such donor–acceptor systems, featuring graphene as an electron donor and Vis-to-NIR electron-acceptor dyads, expands their utility when considered in optoelectronic applications.

Received 8th July 2022,
Accepted 13th September 2022

DOI: 10.1039/d2nr03740h

rsc.li/nanoscale

Open Access Article. Published on 14 September 2022. Downloaded on 7/16/2025 10:45:56 AM.
This article is licensed under a Creative Commons Attribution-NonCommercial 3.0 Unported Licence.

Introduction

Graphene nanosheets can be functionalized through covalent and supramolecular means.[1] In fact, functionalization holds a key role as a methodology for improving or expanding the outstanding inherent properties of graphene. Modification of graphene *via* non-covalent interactions is usually performed in liquid media. However, the forces that stabilize the so-formed ensembles are van der Waals, Coulomb, and/or π–π stacking interactions, which are weak, and the immobilized materials can easily be detached under mild conditions. Conversely, covalent functionalization bears the great advantage of forming stable and robust bonds between graphene and organic species, allowing the evaluation of the produced hybrid materials under more demanding conditions, without the risk of losing the organic addend. In fact, the robustness and quality of such graphene-based hybrid materials allow their fabrication in prototypes and/or participation as individual components in proof-of-concept applications ranging from catalysis and sensing to solar and photoelectrochemical cells.[2–5] In particular for the latter, the functionalization of graphene has progressed and received tremendous importance when graphene is modified with photo- and/or electro-active molecules, enhancing its capabilities in solar energy conversion schemes.[2–5] Significant paradigms to this end feature the covalent incorporation of extended planar π-aromatic systems such as porphyrins[6–12] and phthalocyanines[7–16] with substantial absorption in the Vis and NIR region of the electromagnetic spectrum, respectively. While those chromophores effectively act upon photoirradiation as electron donors when combined with graphene, the situation drastically changes once phthalocyanines are derivatized at the periphery with electron-withdrawing alkylsulfonyl or pyridyl groups and behave as electron acceptors, with graphene being the electron-donating species.[14,17]

[a]*Theoretical and Physical Chemistry Institute, National Hellenic Research Foundation, 48 Vassileos Constantinou Avenue, 11635 Athens, Greece. E-mail: tagmatar@eie.gr; Tel: + 30 210 7273835*
[b]*Department of Chemistry, University of North Texas, 305070 Denton, TX 76203-5017, USA*
[c]*Department of Chemistry, Nagoya University, Nagoya, 464-8602, Japan*
[d]*Department of Chemistry, University of Ioannina, 45110 Ioannina, Greece*
[e]*Department of Physics, Tokyo Metropolitan University, Tokyo 192-0397, Japan*
† Electronic supplementary information (ESI) available. See DOI: https://doi.org/10.1039/d2nr03740h
‡ Equal contributions.

This journal is © The Royal Society of Chemistry 2022

Open Access Article. Published on 14 September 2022. Downloaded on 7/16/2025 10:45:56 AM.
This article is licensed under a Creative Commons Attribution-NonCommercial 3.0 Unported Licence.

Boron azadipyrromethenes (azaBDPs), 4,4-difluoro-4-boron-3a,4a,8-triazo-*s*-indacene, possessing a 12π-electron aromatic structure, are stable and versatile fluorophores, with electron-accepting properties. The substitution of the *meso* carbon of boron dipyrromethene by nitrogen in azaBDPs not only shifts the absorption spectral bands of the latter to the NIR region, normally between 700 and 1200 nm, but also deepens the HOMO–LUMO energy level. The latter justifies the excellent electron-accepting capabilities of azaBDPs, markedly, without the requirement of engineering their molecular structure and introducing substituents (*vide infra* for phthalocyanines). Moreover, the rich chemistry of azaBDPs allows their modular combination with a wide range of photo-active molecular species, such as with parent boron dipyrromethenes[18] and porphyrins (free-base and metallated ones),[19,20] to name a few. Taking advantage of such versatility, designed azaBDPs often carry an aliphatic chain, with the objective to increase solubility in organic solvents, while the presence of a second chromophore enriches the optoelectronic properties of such azaBDP-based dyads. Hence, azaBDPs have been found to participate in energy-related applications,[21,22] acting as primary electron acceptor centers.[23–26]

Having said that, the covalent functionalization of graphene with NIR dyes beyond phthalocyanines,[10,16,17,27,28] with the central objective of the elucidation of photoinduced electron donor–acceptor interactions, has been rarely examined.[29,30] Moreover, chromophore dyads covering the Vis-NIR region, covalently incorporated onto graphene sheets, in which illumination causes graphene to donate electrons, are also scarce, if any at all. Interestingly, supramolecular interactions of azaBDP with non-covalently interacting graphene/Zn-porphyrin yielded an all-supramolecular azaBDP/Zn-porphyrin/graphene nanoensemble, in which graphene acts as a nanoplatform for the aggregation of azaBDP/Zn-porphyrin altering its electronic interactions, while conversely hindering precise conclusions on photophysical events from being reached.[31]

With all the above in mind, it is timely to design and synthesize a dyad with extended absorbance spectral texture in the Vis-NIR region, evidenced by a porphyrin linked to azaBDP, covalently attached to graphene, and screen the photophysical behavior. The prime aim of the current investigation is to explore the electron-donating character of graphene in a hybrid system with a porphyrin-azaBDP, as stimulated by the presence of azaBDP, and to reveal how the presence of this dyad facilitates photoinduced phenomena. Herein, we have (a) synthesized free-base and zinc-metallated porphyrins and conjugated them to NIR absorbing azaBDP derivatives carrying ethylene glycol chains to enhance solubility and (b) anchored them as a dyad under click-chemistry conditions to pre-modified graphene sheets. These newly developed graphene-based hybrid materials were characterized by complementary spectroscopic, thermal, and microscopy imaging techniques. Based on comprehensive photophysical and electrochemical studies, we have been able to identify the occurrence of intrahybrid electron-transfer events upon light illumination, from graphene to azaBDP. These results are of tremendous interest in areas of nanotechnology and energy harvesting applications, in terms that they establish the alter ego nature of graphene, as an electron donor species, while showcasing the effectiveness of photoinduced processes by interfacing with electron-accepting azaBDP-based dyads.

Experimental section

Few layered graphene

Chlorosulfonic acid (50 mL) was added to powder graphite (150 mg), sonicated for 2 h and stirred overnight. Then, the dispersion was added dropwise onto 150 ml of cold water (CAUTION!). The resulting mixture was filtered over a PTFE filter (0.2 μm pore size) and washed several times with distilled water. Before the filter was completely dried, the residual material was transferred to a beaker, NMP (200 mL) was added and the mixture was probe-sonicated (1 h, 100% amplitude of 200 W, 0 °C) and stored in the dark under a nitrogen atmosphere. After 3 days the supernatant was taken, filtrated on a PTFE filter (0.2 μm pore size) and washed with a large amount of methanol, acetone and dichloromethane.

Alkyne-modified graphene (7)

In a typical reaction, 80 mg of few layered graphene were dispersed by sonication in 15 mL of *o*-DCB, under a nitrogen atmosphere. Then, a solution of 4-((trimethylsilyl)ethynyl) aniline (70 mg) in 5 mL of *o*-DCB was added, followed by the quick addition of isoamyl nitrite (1 mL). The reaction mixture was stirred at 120 °C, under N_2, for 7 days with occasional sonication. After cooling down to room temperature, the reaction mixture was diluted with 1 M *n*-Bu_4NF (30 mL) in DMF and stirred overnight. Then it was filtered over a PTFE membrane filter (0.1 μm pore size) and washed with a large amount of DMF and DCM to remove completely any organic residuals. The newly prepared graphene-based hybrid material **7** was obtained as a solid and stored in the dark.

Dipyrromethene-graphene (8)

Diisopropylamine (1.5 mL) was added to a solution of alkyne-modified graphene **7** (60 mg) and dipyrromethane-azide **3** (16 mg) in DMSO (16.8 mL) at room temperature and stirred under a N_2 atmosphere. The reaction was stirred for 14 days with occasional sonication. Then, the reaction mixture was filtered (0.2 μm pore size) and washed extensively with DMF, acetone and DCM. After that period, the reaction mixture was filtered over a PTFE membrane filter (0.1 μm pore size) and washed with a large amount of dichloromethane to remove completely any residual organic matter. The as prepared hybrid material **8** was obtained as a black powder and stored in the dark.

azaBDP-graphene (9)

Boron trifluoride-diethyl etherate (2 mL) was added to a solution of dipyrromethane–graphene hybrid **8** (50 mg) in DCM (10 mL) and diisopropylethylamine (0.5 mL) at room tempera-

Open Access Article. Published on 14 September 2022. Downloaded on 7/16/2025 10:45:56 AM.
This article is licensed under a Creative Commons Attribution-NonCommercial 3.0 Unported Licence.

ture and stirred under a N_2 atmosphere. The reaction was stirred for 48 h with occasional sonication. After that period, the reaction mixture was filtered over a PTFE membrane filter (0.2 μm pore size) and washed with a large amount of MeOH to remove completely any organic residual impurity. The as prepared graphene-based hybrid material **9** was obtained as a black powder and stored in the dark.

H_2P-azaBDP-graphene (10)

Diisopropylamine (1.5 mL) was added to a solution of alkyne-modified graphene **7** (60 mg) and compound **5** (16 mg) in DMSO (16.8 mL) at room temperature and stirred under a N_2 atmosphere. The reaction was stirred for 14 days with occasional sonication. After that period, the reaction mixture was filtered over a PTFE membrane filter (0.1 μm pore size) and washed with a large amount of dichloromethane to remove completely any residual organic matter. The newly prepared graphene-based hybrid material **10** was obtained as a solid and stored in the dark.

ZnP-azaBDP-graphene (11)

Zinc acetate (10 mg) in 2 mL of MeOH was added to a solution of modified graphene **10** (21 mg) in DCM (8 mL) at room temperature and stirred under a N_2 atmosphere. The reaction was stirred for 48 h with occasional sonication. After that period, the reaction mixture was filtered over a PTFE membrane filter (0.2 μm pore size) and washed with a large amount of MeOH to remove completely any residual organic impurity. The newly prepared graphene-based hybrid material **11** was obtained as a solid and stored in the dark.

Results and discussion

The synthetic procedure for the preparation of target materials is based on the synthesis of non-symmetric bis-functionalized azaBDP derivatives, bearing an azide group for click-attachment on alkyne-modified graphene. In this respect, the symmetric diphenolic azadipyrromethene derivative **1** (Fig. 1a), carrying ethylene glycol chains for enhanced solubility, and the corresponding azaBDP **4**, were firstly synthesized.[31] Then, the non-symmetric derivatives were obtained through stepwise mono-condensation reactions. Thus, condensation of **1** with lauric and azidoacetic acids affords azadipyrromethene **3**, while the reaction of **4** with tetraphenyl porphyrin carboxylic acid and azidoacetic acids yields H_2P-azaBDP dyad **5**, which is further zinc-metallated towards the realization of ZnP-azaBDP dyad **6**. The experimental details for all intermediate compounds, together with the full spectroscopic characterization based on NMR and mass spectrometry, are presented in the ESI (Fig. S1–S8).† Next, few-layered graphene was functionalized through a diazotization reaction, employing 4-((trimethylsilyl)ethynyl)aniline and isoamyl nitrite to yield material **7** (Fig. 1b). The click-chemistry reaction between the alkynylated graphene-based material **7** and azide-functionalized chromophores **3** and **5** furnishes **8** and the (H_2P-azaBDP)-graphene hybrid **10**, respectively. A further reaction of **8** with boron trifluoride diethyl etherate results in the formation of the azaBDP-graphene material **9**, while zinc metalation of the porphyrin moiety in **10** yields the (ZnP-azaBDP)-graphene hybrid **11** (Fig. 1b).

Raman spectroscopy provides meaningful information for graphene and its modified analogs, due to the presence of the G band ascribed to vibrations owing to sp^2 hybridized carbon atoms, the D band attributed to vibrations due to sp^3 hybridized carbon atoms, and the 2D band, which is sensitive to the average number of graphene layers.[32,33] The Raman spectrum of **7** shows D, G, and 2D bands, located at 1330, 1580, and 2659 cm^{-1}, respectively (Fig. 2). The 2D band of **7** is found red-shifted by 15 cm^{-1} as compared to that of few layered graphene, meaning that the diazotization functionalization reaction of graphene results in further exfoliation, yielding oligo-layered graphene with an even smaller layer thickness. Furthermore, an increased D/G intensity ratio is found for **7**, as compared to few layered graphene (I_D/I_G = 0.40 for **7**; I_D/I_G = 0.08 for few layered graphene), which is associated with the success of covalent functionalization and the generation of sp^3 carbon atoms. Notably, the D/G intensity ratio of graphene-based materials **8–11** is found practically unaltered as compared to the aforementioned value registered for **7** (Fig. S9†), in accordance with the fact that the click-reaction with **3** and **5** and subsequent complexation and metalation with boron and zinc, respectively, does not further disrupt the graphene framework. The most relevant changes in **8** and **10**, in comparison to **7**, concern the 2D band. In particular, the appreciable enhancement of the 2D band of **8** and **10** compared to **7** is attributed to the additional exfoliation of the modified graphene sheets, resulting from the grafting of the bulky dyes. This is rationalized by considering steric repulsions from the organic addends and the presence of the alkyl chains, reducing graphene self-restacking. Concerning **11**, metalation of the porphyrin does not produce remarkable changes in the Raman spectral D and G bands, in comparison with precursor **10**. Once boron is present in the skeleton of azaBDP in material **9**, a blueshift of the 2D-band of graphene occurs *i.e.* from 2661 cm^{-1} for material **8** to 2697 cm^{-1} for material **9**. In addition, after zinc metalation of **10** yielding **11** a similar blue shift of the 2D-band is also observed. This shift is easy to explain by considering that boron and zinc, in materials **9** and **11**, respectively, strongly interact with graphene.

IR spectroscopy is an indispensable technique to confirm the covalent functionalization of graphene nanosheets. Examining the IR spectrum of material **7**, $-NH_2$ and C–H vibrations are totally absent, while the presence of the alkynyl group has been confirmed by observing the corresponding vibrations at 3286 cm^{-1}. On the other hand, an extra-signature in compound **4**, in comparison with **1** at 1462 cm^{-1} is related to the N–B unit confirming the insertion of boron (Fig. S10†). Finally, the esterification of compound **2** is easily monitored by the appearance of the carbonyl vibration at 1747 cm^{-1}. The azide group in **3** and **5** shows a characteristic vibration band in the corresponding IR spectrum, located at 2111 and

 This journal is © The Royal Society of Chemistry 2022

Open Access Article. Published on 14 September 2022. Downloaded on 7/16/2025 10:45:56 AM.
This article is licensed under a Creative Commons Attribution-NonCommercial 3.0 Unported Licence.

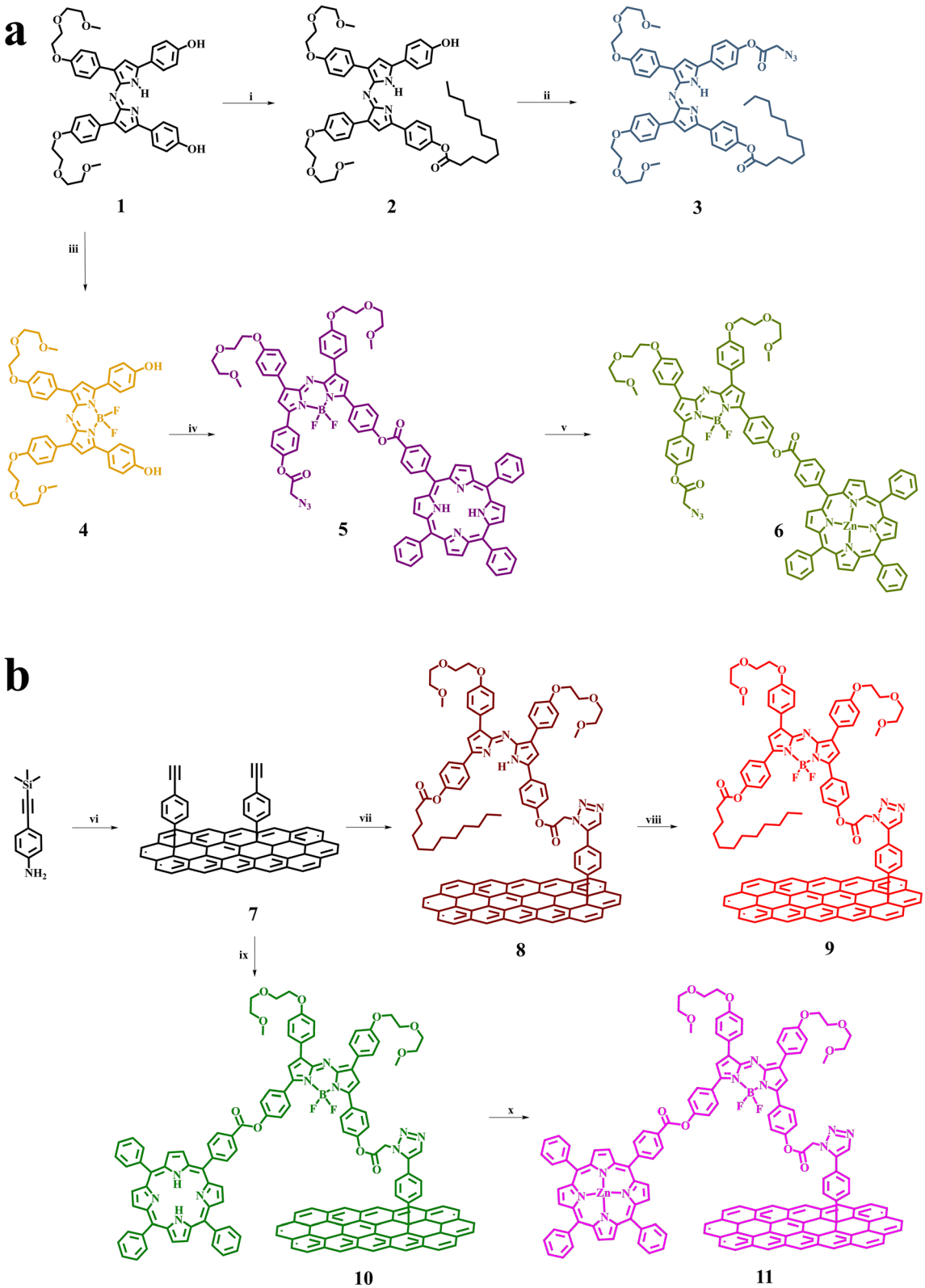

Fig. 1 Synthesis of (a) azaBDP-based dyes **4–6**, and (b) graphene-based hybrids **9–11**. Reaction conditions: (i) EDCI, DMAP, lauric acid, DCM, r.t., 18 h, (ii) azidoacetic acid, EDCI, DMAP, DCM, r.t., 18 h, (iii) $BF_3(OC_2H_5)_2$, DIPEA, DCM, r.t., 48 h, (iv) 4-(10,15,20-triphenylporphyrin-5-yl)benzoic acid, EDCI, DMAP, DCM, r.t., 72 h, and then azidoacetic acid, EDCI, DMAP, DCM, r.t., 72 h, (v) $Zn(OAc)_2$, DCM/MeOH, r.t., 18 h, (vi) Few layered graphene, isoamyl nitrite, *o*-DCB, 120 °C, 7 d, *n*-Bu_4NF, (vii) DIPA, DMSO, **3**, r.t., 14 d, (viii) $BF_3(OC_2H_5)_2$, DIPEA, DCM, r.t., 48 h, (ix) DIPA, DMSO, **5**, r.t., 14 d, and (x) $Zn(OAc)_2$, DCM/MeOH, r.t., 48 h.

Open Access Article. Published on 14 September 2022. Downloaded on 7/16/2025 10:45:56 AM.
This article is licensed under a Creative Commons Attribution-NonCommercial 3.0 Unported Licence.

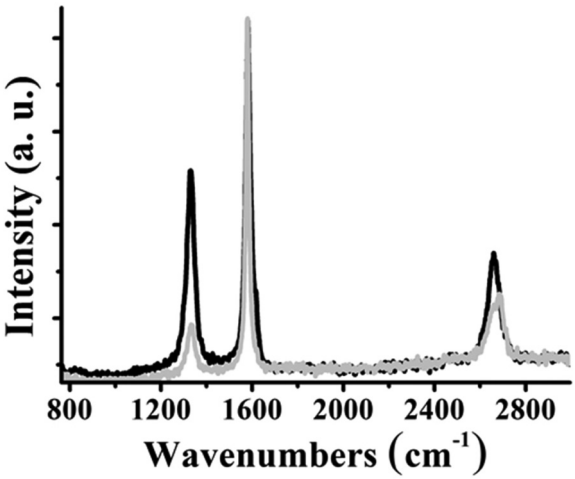

Fig. 2 Raman spectra (633 nm) of few layered graphene (grey) and material **7** (black), normalized at the G band.

2108 cm^{-1}, respectively. Notably, the particular band is absent in the IR spectra of **8** and **10**, highlighting the success of the click-reaction and the effective formation of the corresponding graphene-based hybrid materials. Moreover, the latter not only confirms the covalent incorporation of **3** and **5** on graphene, forming hybrids **8** and **10**, respectively, but also strongly indicates the absence of any non-covalent interactions with those species. This is explained by considering that for the isolation of **8** and **10**, a filtration procedure over the PTFE membrane (0.2 μm pore size) was employed, followed by extensive washing of the powder residue with dichloromethane, which effectively removes any physisorbed species, as confirmed upon examination of the UV-Vis spectrum of the filtrate. In addition, the characteristic strong carbonyl vibrations at 1753 and 1736 cm^{-1} in **3** and 1755 and 1731 cm^{-1} in **5**, accompanied by C–H vibration signatures at 3000–2770 cm^{-1}, are also present in the IR spectra of **8** and **10** (Fig. S10†). Additionally, the IR spectrum of hybrid **11** shows distinguishable carbonyl vibrations, appearing at 1720 and 1713 cm^{-1}, in line with their presence in the IR spectrum of the ZnP-azaBDP dyad **6**.

The degree of functionalization for **7–11** is evaluated by TGA. For **7**, a mass loss of 5.0% is observed in the range 200–600 °C, under nitrogen, suggesting the presence of one organic moiety per 274 carbon atoms of graphene. On the other hand, for **9** the corresponding mass loss is 16.5% (Fig. 3a). This increase in the weight loss is consistent with the introduction of **4** on the graphene backbone, since the former possesses an almost 10-fold increased molecular weight, with regard to that of the organic addend present in **7**. Thus, the organic loading for **9** is calculated to be one moiety per 427 carbon atoms, which suggests that around 50% of all alkynyl groups on **7** are involved in the post-functionalization for **9**. Analogously, the mass loss values of **10** and **11** are 10.5% and 12.5% (Fig. 3b), respectively, which corresponds to one H_2P-azaBDP and one ZnP-azaBDP unit per 1270 carbon atoms, for **10** and **11**, respectively.

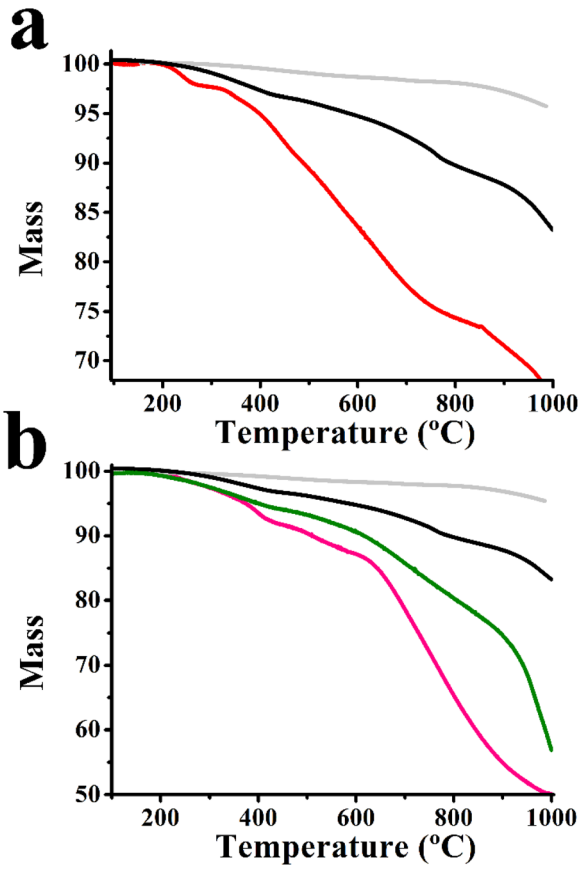

Fig. 3 Thermograms of (a) few layered graphene (grey), **7** (black) and **9** (red), and (b) few layered graphene (grey), **7** (black), **10** (green) and **11** (pink), obtained under N_2.

The morphology of **7–11** was examined by HR-TEM imaging and supported by EDS. The semi-transparent areas in few layered graphene clearly show a few layered material of around several hundred nanometers in size (Fig. 4a). Functionalization of few layered graphene with aryl diazonium salts, yielding **7**, results in new dark regions randomly distributed (Fig. S11a†). Those regions could be related to several phenomena; one possibility is the loss of planarity by the introduction of sp^3 hybridization in the graphene network of **7**, being in harmony with the information obtained by the enhanced D/G intensity ratio in the Raman spectrum. Similarly, dark regions were further confirmed in the images of **8–11**, while the enhanced semi-transparent nature in the images of those hybrids, showing an oligolayered material with fewer nanometer thickness, underscores further exfoliation, reducing the number of stacked layers of graphene, as induced by the incorporation of the covalently attached dyes. Such phenomena are distinguishable in the representative TEM images of **11** (Fig. 4b) as well as of **8–10** (Fig. S11b–d†). Similarly, as described before, the reduction of the number of layers in **8–11** is once again in harmony with the data from the corresponding Raman spectra (Fig. S9†). The EDS of **11** not only supports the incorporation of azaBDP on graphene but

This journal is © The Royal Society of Chemistry 2022

Open Access Article. Published on 14 September 2022. Downloaded on 7/16/2025 10:45:56 AM.
This article is licensed under a Creative Commons Attribution-NonCommercial 3.0 Unported Licence.

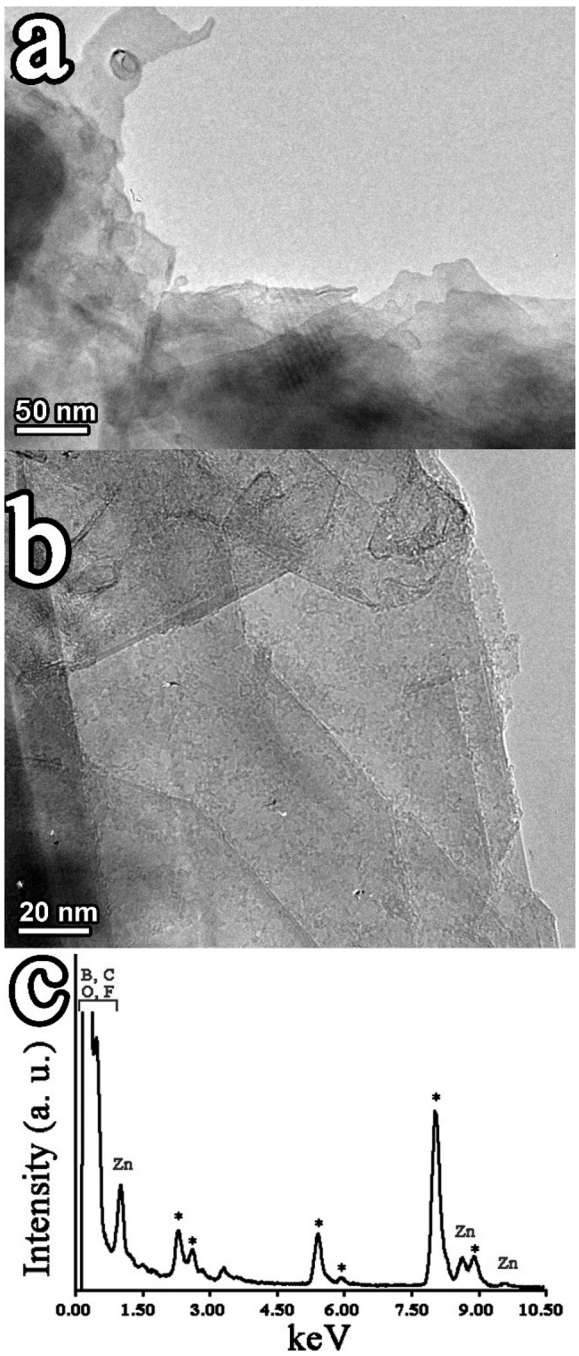

Fig. 4 (a and b) Representative HR-TEM images of few layered graphene, and **11**, respectively. (c) EDS of **11**. Common EDS impurities are marked with * and they are related to the sample holder (Cr), TEM grid (Cu) and sample processing (Si).

also manifests the presence of Zn due to ZnP (Fig. 4c). The corresponding EDS of **8–10** are shown in Fig. S12.†

Material **7** forms unstable dispersions in most organic solvents, while it is marginally soluble in *o*-DCB. On the other hand, **9** shows stable dispersions due to the ethylene glycol and alkyl side chains as parts of the azaBDP unit. After standing for 24 hours, the solubility of **9** in *o*-DCB reaches the values of 0.6 mg mL^{-1} and 0.2 mg mL^{-1} in DMF and dichloromethane. Similarly, **10** and **11** exhibit better solubility in *o*-DCB and DMF, *i.e.* 0.8 and 0.9 mg mL^{-1}, respectively. The latter result signifies the importance of functionalization and gives a clear advantage to **9–11** compared to non-modified graphene, thereby allowing a set of comprehensive photophysical and redox studies in solution to be performed.

Next, UV-Vis-NIR assays were performed in *o*-DCB to shed light on the possible ground state interactions between compounds **4–6** with graphene, within hybrids **9–11**. In the case of azaBDP-graphene **9**, the absorption band due to azaBDP at 686 nm is evident (Fig. 5a). This band is red-shifted by 26 nm compared with that due to azaBDP **4**, which appears at 660 nm. Such a strong shift in the UV-Vis spectrum of **9** is due to a different structural and/or orbital conformation of azaBDP caused by graphene, resulting in an intimate contact/interaction between the π–π orbitals of the two species in the ground state. Such π–π interactions are known to create a bandgap in graphene.[32] The appearance of a band in the photoluminescence spectrum of azaBDP-graphene **9** at 716 nm, upon excitation at 686 nm (Fig. 5b) guarantees the successful integration of boron in the azadipyrromethene skeleton. Then, a considerable depression of the emission of **9**, in

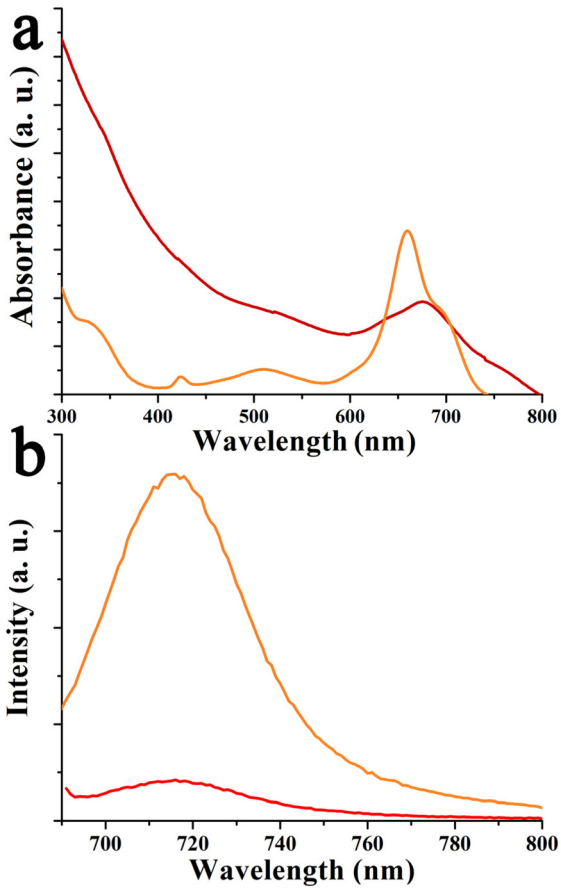

Fig. 5 (a) Absorption and (b) fluorescence spectra (λ_{exc} 686 nm) of **4** (orange) and **9** (red), in *o*-DCB.

Open Access Article. Published on 14 September 2022. Downloaded on 7/16/2025 10:45:56 AM.
This article is licensed under a Creative Commons Attribution-NonCommercial 3.0 Unported Licence.

comparison with azaBDP **4**, is observed, for samples possessing equal optical concentrations at the excitation wavelength, suggesting the occurrence of excited state events in hybrid **9**.[34–36]

The spectral properties of relatively complex bis-fluorophore appended graphene were investigated, as shown in Fig. 6 and Fig. S13.† Special attention was given to probing spectral perturbation of the individual chromophores of the dyads upon grafting on graphene, excited-state energy, and electron transfer within the porphyrin-azaBDP dyads as a function of metal ion in the porphyrin cavity, and the role of graphene in modulating the luminescence properties. Fig. 6a shows the absorption spectra of ZnP-azaBDP **6** and (ZnP-azaBDP)-graphene hybrid **11**, along with their control compounds azaBDP **4** and ZnP. The spectra are normalized to the ZnP Soret band for comparison purposes. The control ZnP was characterized by peaks at 425, 551, and 590 nm. In the ZnP-azaBDP dyad **6**, the peaks corresponding to ZnP did not reveal significant changes, suggesting a lack of ground state interactions between the two chromophores. In the case of (ZnP-azaBDP)-graphene hybrid **11**, while the ZnP absorption bands did not show appreciable changes, the azaBDP absorption peak revealed a red-shift similar to that discussed earlier for azaBDP-graphene **9** (Fig. 5). This was also the case for (H_2P-azaBDP)-graphene hybrid **10**. That is, minimal spectral shifts for the porphyrin peaks and notable changes for azaBDP were witnessed. In fact, the azaBDP-centred absorption band in **10** appeared at 690 nm, with a 30 nm shift from that observed for azaBDP **4** (Fig. S13a†). These spectral results show stronger interactions between spatially close azaBDP with the graphene surface, as compared to distantly positioned porphyrin entities within the hybrids.

Then, the fluorescence of these materials was systematically investigated. As shown in Fig. 6b, ZnP revealed two emission

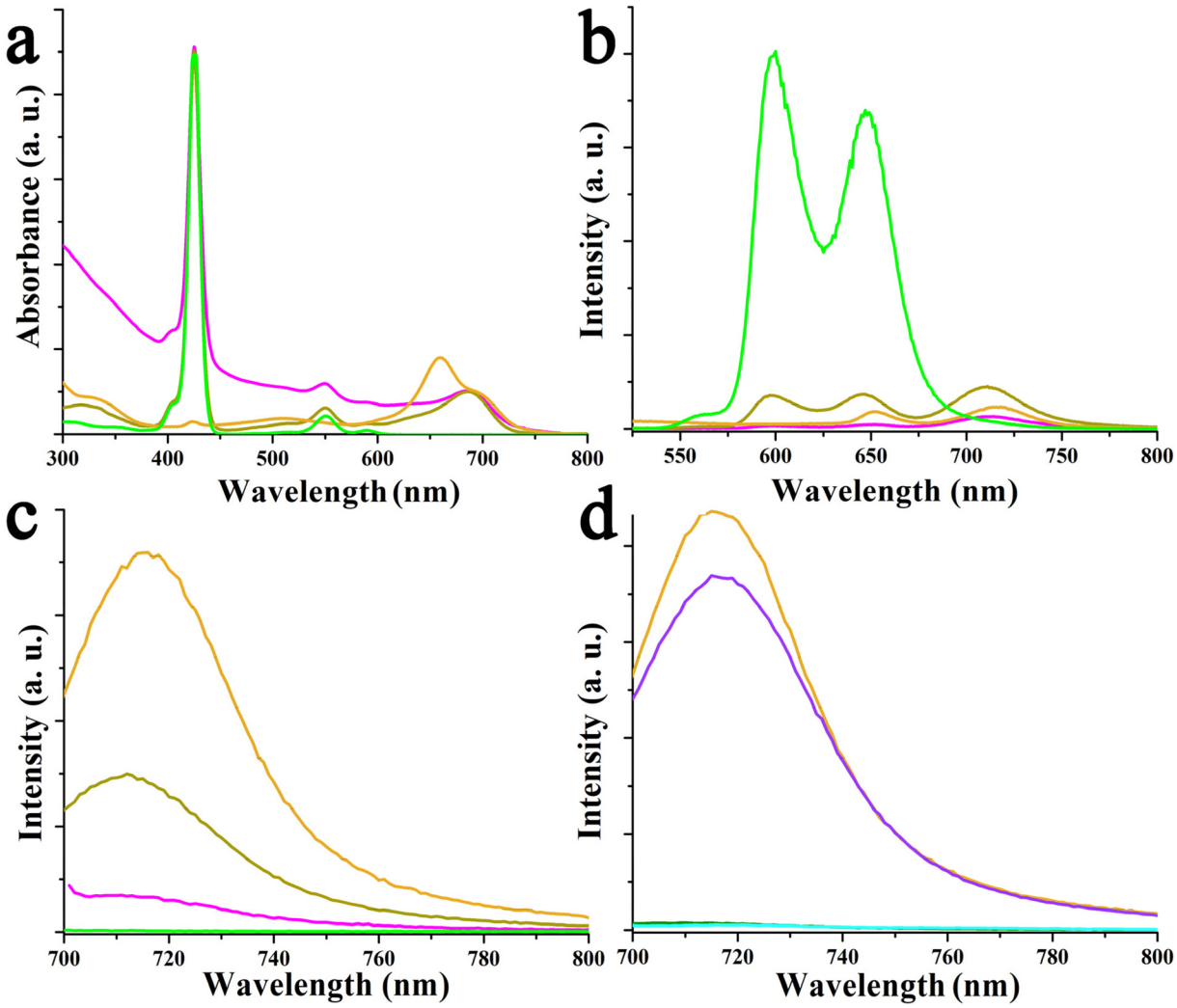

Fig. 6 (a) UV-Vis spectra of azaBDP **4** (orange), ZnP (green), ZnP-azaBDP **6** (olive), and (ZnP-azaBDP)-graphene **11** (pink). Fluorescence spectra of azaBDP **4** (orange), ZnP (green), ZnP-azaBDP **6** (olive), and (ZnP-azaBDP)-graphene **11** (pink), upon excitation at (b) 424 nm and (c) 686 nm. (d) Fluorescence spectra of azaBDP **4** (orange), H_2P (cyan), H_2P-azaBDP **5** (purple), and (H_2P-azaBDP)-graphene **10** (dark green), upon excitation at 686 nm. All measurements are in *o*-DCB.

 This journal is © The Royal Society of Chemistry 2022

Open Access Article. Published on 14 September 2022. Downloaded on 7/16/2025 10:45:56 AM.
This article is licensed under a Creative Commons Attribution-NonCommercial 3.0 Unported Licence.

bands at 600 and 648 nm, upon excitation at 424 nm, corresponding to the Soret band maximum. Upon appending azaBDP, the resulting ZnP-azaBDP dyad **6** revealed notable changes. First, both the porphyrin-centered emission peaks revealed over 90% quenching, without any shifts in the peak position, along with a new peak at 714 nm, corresponding to azaBDP, suggesting the occurrence of energy transfer. This is reasonable, as there is a substantial overlap between ZnP emission and azaBDP absorption,[19] a primary condition for energy transfer to occur.[35] As a control, an equimolar concentration of azaBDP **4** was also excited at 424 nm, wherein the observed emission intensity was less than 50% of what was observed for **6**, suggesting that the 714 nm peak has contributions of energy transfer from ^{1}ZnP*. Finally, in the (ZnP-azaBDP)-graphene hybrid **11**, the ZnP emission was quantitatively quenched, while azaBDP emission was quenched by over 75%. Similar observations, however, with higher quenching, were observed in the case of the (H_2P-azaBDP)-graphene hybrid **10**, as shown in Fig. S13b.† The H_2P emission was quenched at over 98% in the azaBDP-H_2P dyad **5**, with the appearance of an azaBDP emission peak in the 714 nm region, indicating the occurrence of energy transfer. Furthermore, almost quantitative quenching of both H_2P and azaBDP peaks in the case of the (H_2P-azaBDP)-graphene hybrid **10** was observed.

In dyads H_2P-azaBDP **5** and ZnP-azaBDP **6** as well as the corresponding hybrids (H_2P-azaBDP)-graphene **10** and (ZnP-azaBDP)-graphene **11**, the ^{1}azaBDP*, formed by direct excitation or as the product of energy transfer from the porphyrin moiety, could undergo additional photochemical events such as charge transfer due to facile reduction of azaBDP and relatively easier oxidation of porphyrin (*vide infra*), and/or with graphene. To probe the possibility of such photo-events, azaBDP in both dyads, H_2P-azaBDP **5** and ZnP-azaBDP **6**, as well as hybrids (H_2P-azaBDP)-graphene **10** and (ZnP-azaBDP)-graphene **11**, was directly excited and compared with the fluorescence intensity of individual azaBDP **4** (Fig. 6c and d). In the case of ZnP-derived systems, ^{1}azaBDP* fluorescence was quenched by nearly 60% in ZnP-azaBDP dyad **6**. The presence of graphene in (ZnP-azaBDP)-graphene hybrid **11** further quenched the fluorescence over to 90% (Fig. 6c). Notably, at an excitation wavelength of 686 nm, no emission of ZnP was observed. These results suggest excited-state events originating from ^{1}azaBDP* involving ZnP in both **6** and **11**, and in the latter case also involving graphene. The situation was somewhat different in the H_2P-derived systems. The ^{1}azaBDP* quenching in H_2P-azaBDP dyad **5** was only marginal, being only 14%, while in (H_2P-azaBDP)-graphene hybrid **10**, such quenching was quantitative (Fig. 6d). No emission of H_2P at an excitation wavelength of 686 nm was observed. These quenching studies reveal a lack of major photochemical events from ^{1}azaBDP* to H_2P in H_2P-azaBDP **5**, while a major quenching in the case of **10** arises as a result of its interaction with graphene.

Electrochemical investigations using both CV, for verifying reversibility, and DPV, for accurate peak potential assignment, were performed in *o*-DCB. No faradaic process could be registered for graphene during both anodic and cathodic potential scans, but only small non-faradaic currents were observed. This is reasonable as graphene is expected to show material type behavior rather than the molecular type. As shown in Fig. 7a, the first reduction of azaBDP **4** was registered at −0.44 V *vs.* Ag/AgCl (fully reversible on the CV time scale) and two oxidations, at 0.86 and 1.30 V. The reduction potential of **4** compares favourably with those of the traditionally used electron acceptors such as quinone and C_{60}.[37–39] In the case of ZnP-azaBDP **6**, reductions at −0.36, −1.30, and −1.55 V were observed (Fig. 7c). From control experiments, it can be seen that the first reduction at −0.36 originated from azaBDP, while

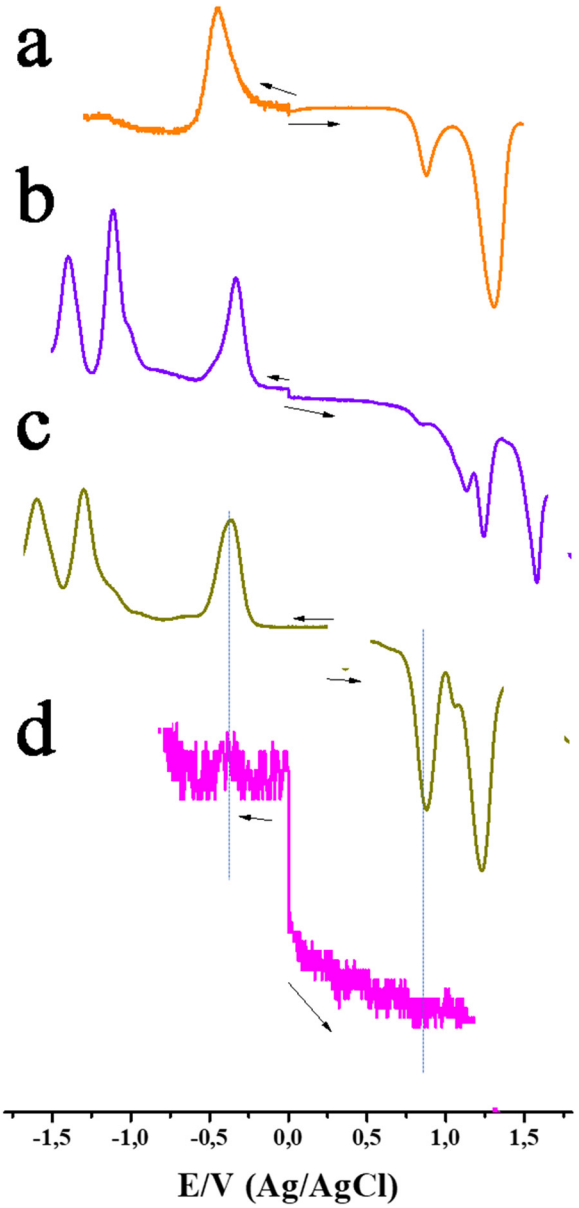

Fig. 7 DPVs of azaBDP **4** (orange), H_2P-azaBDP dyad **5** (purple), ZnP-azaBDP dyad **6** (olive) and (ZnP-azaBDP)-graphene hybrid **11** (pink), in *o*-DCB containing 0.1 M (TBA)ClO_4 as the electrolyte.

Open Access Article. Published on 14 September 2022. Downloaded on 7/16/2025 10:45:56 AM.
This article is licensed under a Creative Commons Attribution-NonCommercial 3.0 Unported Licence.

the latter two originated from ZnP reduction, which were possible to assign. At the anodic side, oxidation was observed at 0.89 and 1.23 V for ZnP-azaBDP **6**, both corresponding to ZnP. The oxidation peak present at 0.86 V for **4** disappeared in dyad **6**, suggesting that it was due to the oxidation of the –OH groups in azaBDP **4**. In the case of H_2P-azaBDP dyad **5**, reductions at −0.34 (due to azaBDP) and at −1.11 and −1.39 V (both due to H_2P) were registered (Fig. 7b). At the anodic side, oxidation was observed at 1.14 and 1.24 V (due to H_2P) and at 1.57 V (due to azaBDP). In the cases of graphene bearing hybrids **9–11**, although most of the peaks were visible, the currents were much smaller due to their limited solubility and the large molecular weight (slow diffusion) of the hybrids. As an example, a representative DPV of **11** is shown in Fig. 7d.

An energy level diagram was subsequently established, using spectral and electrochemical results (Fig. 8). From this, the thermodynamic feasibility of singlet–singlet energy transfer from $^1H_2P^*$ and $^1ZnP^*$ to azaBDP is obvious. Charge transfer is also a possibility, however, this could be considered a minor path, due to the aforementioned discussions. The energy transfer product, ^{1}azaBDP*, or the same species formed by direct excitation of azaBDP, could undergo electron transfer involving H_2P and ZnP to yield $H_2P^{\bullet+}$-azaBDP$^{\bullet-}$ and ZnP$^{\bullet+}$-azaBDP$^{\bullet-}$, more so in the case of ZnP-azaBDP due to facile oxidation of ZnP, both in the dyad and hybrid. Additionally, in the case of the (H_2P-azaBDP)-graphene hybrid **10** and the (ZnP-azaBDP)-graphene hybrid **11**, the ^{1}azaBDP* entity could have an additional deactivation path *via* charge transfer involving graphene. The quantitative quenching observed in the case of hybrids (H_2P-azaBDP)-graphene **10** and (ZnP-azaBDP)-graphene **11** draws support for this mechanism. It may also be mentioned here that no fluorescence lifetime for hybrids **10** and **11** could be recorded using the time-correlated single-photon counting method (<200 ps), suggesting that the observed quenching is indeed dynamic and not static.

Spectroelectrochemical studies on the control chromophores were reported earlier by us.[23] The one-electron reduced product of azaBDP **4**, namely azaBDP$^{\bullet-}$, is characterized by peaks at 446 nm and another peak in the NIR region at 823 nm (Fig. S14†). Similarly, $H_2P^{\bullet+}$ and ZnP$^{\bullet+}$ are characterized by new peaks in the 650–670 nm range.[37] These will serve as diagnostic proof of electron transfer in dyads **5** and **6** and the corresponding hybrids with graphene **10** and **11**, respectively.

Finally, femtosecond transient absorption (fs-TA) spectral studies were performed to secure evidence of energy and charge transfer processes. First, the transient features of control chromophores were recorded (Fig. S15†). The fs-TA features of azaBDP **4** involved excited state absorption (ESA) peaks of ^{1}azaBDP* at 456, 776, and 885 nm. Ground state bleach (GSB) and stimulated emission (SE) peaks were also observed at their expected absorption peak maxima around 650 and 712 nm. The ^{1}ZnP* formed upon excitation of ZnP revealed ESA peaks at 458, 575, 612, 684, and 1290 nm. GSB peaks at 548 and 588 nm, and SE peaks at 592 and 650 nm were observed. Decay and recovery of the positive and negative peaks were accompanied by new peaks at 480 and 850 nm corresponding to ^{3}ZnP*, a product of intersystem crossing.

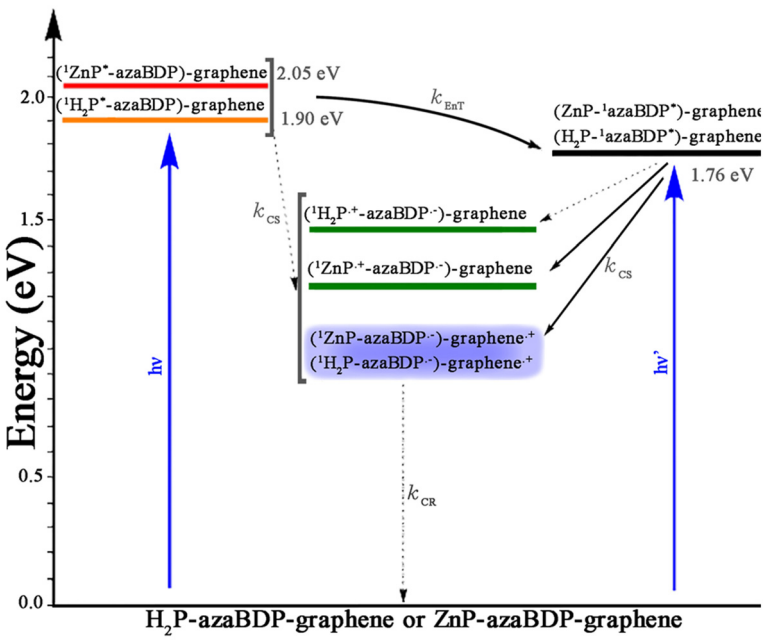

Fig. 8 Energy level diagram depicting different photochemical events occurring in hybrids (H_2P-azaBDP)-graphene **10** and (ZnP-azaBDP)-graphene **11** as a function of the excitation wavelength. Solid arrows indicate most likely processes, while dashed arrows indicate less likely processes. The energy of the (H_2P-azaBDP)-graphene hybrid **10** and (ZnP-azaBDP)-graphene hybrid **11** is largely an assumed value based on quenching properties as no anodic process corresponding to graphene oxidation was possible due to the large size and slow diffusion of the hybrid materials.

 This journal is © The Royal Society of Chemistry 2022

Open Access Article. Published on 14 September 2022. Downloaded on 7/16/2025 10:45:56 AM.
This article is licensed under a Creative Commons Attribution-NonCommercial 3.0 Unported Licence.

Similar observations were also made in the case of H_2P, however, decay/recovery of the positive and negative peaks of $^1H_2P^*$ resulting in $^3H_2P^*$ was slow, consistent with the longer singlet excited lifetime of H_2P, being ~10 ns.

Next, dyads H_2P-azaBDP **5** and ZnP-azaBDP **6** were investigated to seek energy transfer from excited porphyrin to azaBDP by exciting at 424 nm corresponding to the porphyrin Soret band. As shown in Fig. 9, the ^{1}ZnP* formed within the first ps revealed main ESA peaks at 485 and 714 nm, along with a GSB peak at 548 nm. A very small contribution of the SE peak at 590 nm was observed suggesting that this state is involved in the additional photophysical events. Decay and recovery of the ESA and GSB peak were associated with a new signal at 682 nm, expected for the GSB of ^{1}azaBDP* accompanied by a small blue-shift of 4 nm of the ESA peak at 485 nm and additional broad absorption features at 775 nm attributable to the ESA peak ^{1}azaBDP*. These results directly provide evidence of singlet–singlet energy transfer in the dyad.[20] From the time profile of the 682 nm peak (Fig. 9a and c), a rate of energy transfer, $k_{ENT} = 4.6 \times 10^{10}$ s^{-1}, was recorded. The recovery of this also provided the lifetime of ^{1}azaBDP* to be 396 ps. This relatively short lifetime suggests its participation in subsequent photochemical events, likely thermodynamically feasible electron transfer leading to the ZnP$^{\bullet+}$-azaBDP$^{\bullet-}$ charge-separated state. A close examination of the transient spectra at a higher delay time clearly shows the development of a new peak in the 610 nm range, characteristic of ZnP$^{\bullet+}$. The estimated electron transfer rate constant was found to be ~1.6×10^{10} s^{-1}. As shown in Fig. 9b and d, such an excitation transfer process was also witnessed in the H_2P-azaBDP dyad **5**, wherein decay and recovery of the ESA/GSB peak were associated with a new SE peak at 682 nm, corresponding to ^{1}azaBDP*. From the time profile, a rate constant for energy transfer, $k_{ENT} = 1.3 \times 10^{10}$ s^{-1}, was obtained. Recovery of the signal yielded a lifetime of ^{1}azaBDP* 750 ps, almost double that obtained for the ZnP-azaBDP dyad **6**. Predictably, no new peak associated with $H_2P^{\bullet+}$ in the 600–700 nm range was observed, suggesting a lack of electron transfer between

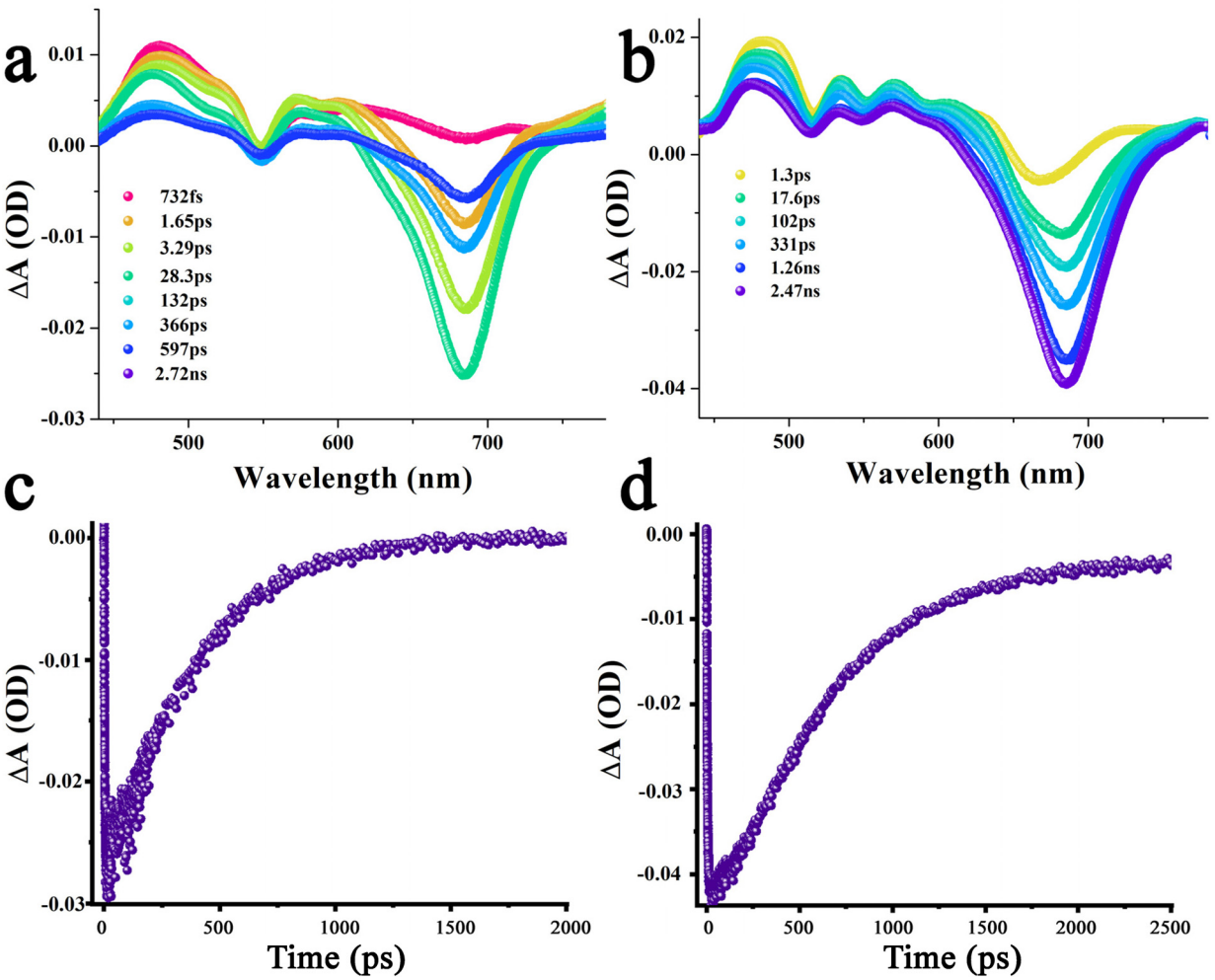

Fig. 9 fs-TA spectra at the indicated delay time of (a) ZnP-azaBDP dyad **6**, and (b) H_2P-azaBDP dyad **5**, in *o*-DCB. The samples were excited at 424 nm. The profile of the 682 nm peak corresponding to ^{1}azaBDP* in the ZnP-azaBDP dyad **6** and the H_2P-azaBDP dyad **5** is shown in (c) and (d), respectively.

Open Access Article. Published on 14 September 2022. Downloaded on 7/16/2025 10:45:56 AM.
This article is licensed under a Creative Commons Attribution-NonCommercial 3.0 Unported Licence.

^{1}azaBDP* and H_2P. These observations agree well with earlier discussed fluorescence spectral data and energy level diagrams.

Transient spectral features of graphene bearing hybrids **9–11** were also subsequently performed. As shown in Fig. 10a, in azaBDP-graphene **9**, excitation corresponding to the azaBDP peak maxima also revealed the expected phonon peaks of graphene, due to its broad absorbance along with spectral features covering both ESA/GSA peaks of azaBDP. Importantly, although weak due to the low sensitivity of the detector in the wavelength range, a clear peak in the 835 nm range was present. The peak position agreed well with the absorption spectrum of azaBDP$^{\bullet-}$ shown in Fig. S14,† providing direct evidence of charge transfer in hybrid **9**. As expected for closely interacting entities, such transient features were short-lived. In less than 1 ps such spectral features vanished, suggesting the occurrence of ultrafast charge transfer and recombination in **9**. Similar trends were also observed for hybrids (H_2P-azaBDP)-graphene **10** and (ZnP-azaBDP)-graphene **11**, when excited at 424 or 650 nm. As shown in Fig. 10b and c, when the samples were excited at a peak position corresponding to the porphyrin Soret band, the ESA/GSA peaks of H_2P and ZnP and graphene phonon peaks simultaneously appeared, exhibiting a rather complex transient spectrum. Additional difficulties were also encountered due to shifting positions of the strong graphene phonon peaks and comparatively low absorptivity of the transient bands of porphyrin and azaBDP. Nevertheless, both hybrids **10** and **11** revealed a peak in the 835 nm range expected for azaBDP$^{\bullet-}$ demonstrating successful short-lived, ultrafast charge transfer in these hybrids.

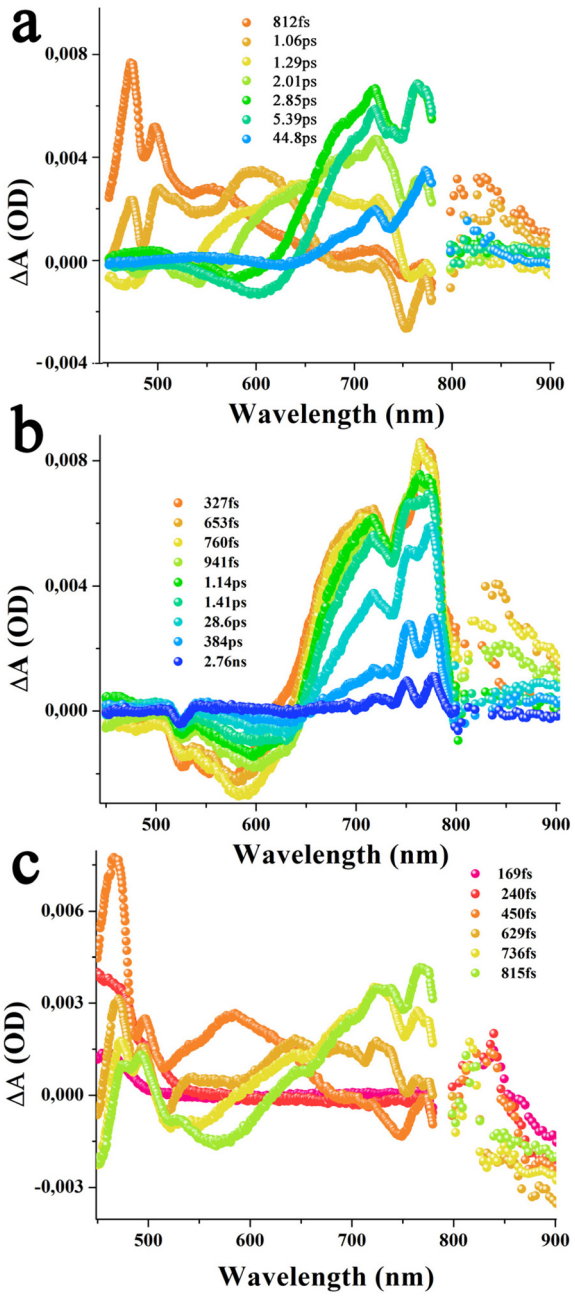

Fig. 10 fs-TA spectra at the indicated delay times of (a) azaBDP-graphene material **9** (λ_{exc} 650 nm), (b) (ZnP-azaBDP)-graphene hybrid **11** (λ_{exc} 424 nm), and (c) (H_2P-azaBDP)-graphene hybrid **10** (λ_{exc} 424 nm), in *o*-DCB.

Conclusions

Few layered graphene was covalently functionalized with dyads H_2P-azaBDP **5** and ZnP-azaBDP **6** yielding hybrids (H_2P-azaBDP)-graphene **10** and (ZnP-azaBDP)-graphene **11**, respectively. The covalent functionalization ensures the absence of aggregations in the newly formed hybrid materials, bringing graphene and chromophore dyads in intimate contact and revealing interesting photophysical properties that were previously masked when the species were non-covalently interacting.[29] Interestingly, both hybrids (H_2P-azaBDP)-graphene **10** and (ZnP-azaBDP)-graphene **11** managed energy transfer processes between the chromophores, however, only in the latter **11** charge separation between the chromophores was registered, yielding (ZnP$^{\bullet+}$-azaBDP$^{\bullet-}$)-graphene. Conversely, upon illumination, graphene acted as an electron donor, yielding (H_2P-azaBDP$^{\bullet-}$)-graphene$^{\bullet+}$ and (ZnP-azaBDP$^{\bullet-}$)-graphene$^{\bullet+}$ charge-separated states, establishing its dual nature, as donating and accepting electrons, once properly functionalized. All in all, the development of such hybrid systems, featuring graphene as an electron donor interfaced with Vis-to-NIR absorbing porphyrin-azaBDP dyads, expands the utility of graphene in energy harvesting applications.

Author contributions

Ruben Canton-Vitoria and Ajyal Z. Alsaleha had an equal contribution to this work.

Conflicts of interest

There are no conflicts to declare.

This journal is © The Royal Society of Chemistry 2022

Open Access Article. Published on 14 September 2022. Downloaded on 7/16/2025 10:45:56 AM.
This article is licensed under a Creative Commons Attribution-NonCommercial 3.0 Unported Licence.

Acknowledgements

This project has received funding from the European Union's Horizon 2020 research and innovation programme under the Marie Sklodowska-Curie grant agreement No. 642742. Support by JSPS KAKENHI (20H02572) and JST CREST (No. JPMJCR20B1) is acknowledged. The authors are thankful to the National Science Foundation for the support of this work.

References

1 A. Stergiou, R. Canton-Vitoria, M. Psarrou, S. Economopoulos and N. Tagmatarchis, Functionalized graphene and targeted applications – highlighting the road from chemistry to applications, *Prog. Mater. Sci.*, 2020, **114**, 100683.

2 A. Stergiou, G. Pagona and N. Tagmatarchis, Donor–acceptor graphene-based hybrid materials facilitating photoinduced electron-transfer reactions, *Beilstein J. Nanotechnol.*, 2014, **5**, 1580–1589.

3 V. Georgakilas, J. N. Tiwari, K. C. Kemp, J. A. Perman, A. B. Bourlinos, K. S. Kim and R. Zboril, Noncovalent functionalization of graphene and graphene oxide for energy rmaterials, biosensing, catalytic, and biomedical applications, *Chem. Rev.*, 2016, **116**, 5464–5519.

4 K. Dirian, M. A. Herranz, G. Katsukis, J. Malig, L. R. Perez, C. Romero-Nieto, V. Strauss, N. Martin and D. M. Guldi, Low dimensional nanocarbons–chemistry and energy/electron transfer reactions, *Chem. Sci.*, 2013, **4**, 4335–4353.

5 J. Malig, N. Jux and D. M. Guldi, Toward multifunctional wet chemically functionalized graphene—integration of oligomeric, molecular, and particulate building blocks that reveal photoactivity and redox activity, *Acc. Chem. Res.*, 2013, **46**, 53–64.

6 D. Dasler, R. Schäfer, M. Minameyer, J. Hitzenberger, F. Hauke, T. Drewello and A. Hirsch, Direct covalent coupling of porphyrins to graphene, *J. Am. Chem. Soc.*, 2017, **139**, 11760–11765.

7 A. Wang, W. Yu, Z. Huang, F. Zhou, J. Song, Y. Song, L. Long, M. P. Cifuentes, M. G. Humphrey, L. Zhang, J. Shao and C. Zhang, Covalent functionalization of reduced graphene oxide with porphyrin by means of diazonium chemistry for nonlinear optical performance, *Sci. Rep.*, 2016, **6**, 23325.

8 N. Karousis, A. Sandanayaka, T. Hasobe, S. Economopoulos, E. Sarantopoulou and N. Tagmatarchis, Graphene oxide with covalently linked porphyrin antennae: Synthesis, characterization and photophysical properties, *J. Mater. Chem.*, 2011, **21**, 109–117.

9 A. Wang, W. Yu, Z. Xiao, Y. Song, L. Long, M. P. Cifuentes, M. G. Humphrey and C. Zhang, A 1,3-dipolar cycloaddition protocol to porphyrin-functionalized reduced graphene oxide with a push-pull motif, *Nano Res.*, 2015, **8**, 870–886.

10 N. Karousis, J. Ortiz, K. Ohkubo, T. Hasobe, S. Fukuzumi, Á. Sastre-Santos and N. Tagmatarchis, Zinc phthalocyanine–graphene hybrid material for energy conversion: synthesis, characterization, photophysics, and photoelectrochemical cell preparation, *J. Phys. Chem. C*, 2012, **116**, 20564–20573.

11 T. Umeyama, J. Mihara, N. Tezuka, Y. Matano, K. Stranius, V. Chukharev, N. V. Tkachenko, H. Lemmetyinen, K. Noda, K. Matsushige, T. Shishido, Z. Liu, K. Hirose-Takai, K. Suenaga and H. Imahori, Preparation and photophysical and photoelectrochemical properties of a covalently fixed porphyrin–chemically converted graphene composite, *Eur. J. Chem.*, 2012, **18**, 4250.

12 T. Umeyama, T. Hanaoka, J. Baek, T. Higashino, F. Abou-Chahine, N. V. Tkachenko and H. Imahori, Remarkable dependence of exciplex decay rate on through-space separation distance between porphyrin and chemically converted graphene, *J. Phys. Chem. C*, 2016, **120**, 28337.

13 M. Barrejón, A. Primo, M. Gómez-Escalonilla, J. Fierro, H. García and F. Langa, Covalent functionalization of N-doped graphene by N-alkylation, *Chem. Commun.*, 2015, **51**, 16916–16919.

14 M.-E. Ragoussi, G. Katsukis, G. A. Roth, J. Malig, G. de la Torre, G. D. M. Guldi and T. Torres, Electron-donating behavior of few-layer graphene in covalent ensembles with electron-accepting phthalocyanines, *J. Am. Chem. Soc.*, 2014, **136**, 4593–4593.

15 Y. Wang, A. Zhou, Y. Jiang, X. Chen and J. He, Tetraaminozinc phthalocyanine covalently bound to benzoic acid-functionalized graphene composites for highly efficient visible light photocatalytic activities, *RSC Adv.*, 2015, **5**, 37823–37829.

16 A. Wang, J. Ye, M. G. Humphrey and C. Zhang, Graphene and carbon-nanotube nanohybrids covalently functionalized by porphyrins and phthalocyanines for optoelectronic properties, *Adv. Mater.*, 2018, **30**, 1705704–1705713.

17 L. Wibmer, L. Lourenço, A. Roth, G. Katsukis, M. Neves, J. Cavaleiro, J. Tomé, T. Torres and D. Guldi, Decorating graphene nanosheets with electron accepting pyridylphthalocyanines, *Nanoscale*, 2015, **7**, 5674–5682.

18 V. Bandi, F. D'Souza, H. Gobeze and F. D'Souza, Multistep energy and electron transfer in a "V-Configured" supramolecular BODIPY-azabodipy-fullerene triad: Mimicry of photosynthetic antenna reaction-center events, *Chem. – Eur. J.*, 2014, **21**, 2669–2679.

19 F. D'Souza, A. Amin, M. El-Khouly, N. Subbaiyan, M. Zandler and S. Fukuzumi, Control over photoinduced energy and electron transfer in supramolecular polyads of covalently linked azaBODIPY-Bisporphyrin 'Molecular Clip' hosting fullerene, *J. Am. Chem. Soc.*, 2011, **134**, 564–664.

20 S. Pascal, L. Bucher, N. Desbois, C. Bucher, C. Andraud and C. Gros, Synthesis, electrochemistry, and photophysics of Aza-BODIPY porphyrin dyes chemistry, *Chem. – Eur. J.*, 2016, **22**, 4971–4979.

21 Y. Ge and D. F. O'Shea, Azadipyrromethenes: from traditional dye chemistry to leading edge applications, *Chem. Soc. Rev.*, 2016, **45**, 3846–3864.

22 M. E. El-Khouly, S. Fukuzumi and F. D'Souza, Photosynthetic antenna–reaction center mimicry by using

Open Access Article. Published on 14 September 2022. Downloaded on 7/16/2025 10:45:56 AM.
This article is licensed under a Creative Commons Attribution-NonCommercial 3.0 Unported Licence.

boron dipyrromethene sensitizers, *ChemPhysChem*, 2014, **15**, 30–47.

23 A. Amin, M. El-Khouly, N. Subbaiyan, M. Zandler, M. Supur, S. Fukuzumi and F. D'Souza, Syntheses, electrochemistry, and photodynamics of ferrocene–azadipyrromethane donor–acceptor dyads and triads, *J. Phys. Chem. A*, 2011, **115**, 9810–9819.

24 H. Lim, S. Seo, S. Pascal, Q. Bellier, S. Rigaut, C. Park, H. Shin, O. Maury, C. Andraud and E. Kim, NIR Electrofluorochromic properties of aza-boron-dipyrromethene dyes, *Sci. Rep.*, 2016, **6**, 18867.

25 Y. Kage, S. Kang, S. Mori, M. Mamada, C. Adachi, D. Kim, H. Furuta and S. Shimizu, An electron–accepting aza–BODIPY–based donor–acceptor–donor architecture for bright NIR emission, *Chem. – Eur. J.*, 2021, **27**, 5259–5267.

26 Y. Xu, M. Zhao, L. Zou, L. Wu, M. Xie, T. Yang, S. Liu, W. Huang and Q. Zhao, Highly stable and multifunctional aza-BODIPY-based phototherapeutic agent for anticancer treatment, *ACS Appl. Mater. Interfaces*, 2018, **10**, 44324–44335.

27 J. Pan, Y. Yang, W. Fang, W. Liu, K. Le, D. Xu and X. Li, Fluorescent phthalocyanine-graphene conjugate with enhanced NIR absorbance for imaging and multi-modality therapy, *ACS Appl. Nano Mater.*, 2018, **1**, 2785–2795.

28 G. Neelgund and A. Oki, Cobalt phthalocyanine-sensitized graphene–ZnO composite: An efficient near-infrared-Active photothermal agent, *ACS Omega*, 2019, **4**, 5696–5704.

29 A. Roth, C. Schierl, A. Ferrer-Ruiz, M. Minameyer, L. Rodríguez-Pérez, C. Villegas, M. Ángeles-Herranz, N. Martín and D. M. Guldi, Low-dimensional carbon allotropes: Ground- and excited-state charge transfer with NIR-absorbing heptamethine cyanine, *Chem*, 2017, 164–173.

30 K. C. Prousis, R. Canton-Vitoria, G. Pagona, M. Goulielmaki, V. Zoumpourlis, N. Tagmatarchis and T. Calogeropoulou, New cationic heptamethine cyanine-graphene hybrid materials, *Dyes Pigm.*, 2020, **175**, 108047.

31 G. Rotas, M. B. Thomas, R. Canton-Vitoria, F. D'Souza and N. Tagmatarchis, Preparation, photophysical and electrochemical evaluation of an azaborondipyrromethene/zinc porphyrin/graphene supramolecular nanoensemble, *Chem. – Eur. J.*, 2020, **26**, 6652–6661.

32 A. C. Ferrari, J. C. Meyer, V. Scardaci, C. Casiraghi, M. Lazzeri, F. Mauri, S. Piscanec, D. Jiang, K. S. Novoselov, S. Roth and A. K. Geim, Raman spectrum of graphene and graphene layers, *Phys. Rev. Lett.*, 2006, **97**, 187401–187404.

33 A. Gupta, G. Chen, P. Joshi, S. Tadigadapa and P. C. Eklund, Raman scattering from high-frequency phonons in supported n-graphene layer films, *Nano Lett.*, 2006, **6**, 2667–2673.

34 G. Bottari, A. A. Herranz, L. Wibmer, M. Volland, L. Rodriguez-Perez, K. M. Guldi, A. Hirsch, N. Martin, F. D'Souza and T. Torres, Chemical functionalization and characterization of graphene-based materials, *Chem. Soc. Rev.*, 2017, **46**, 4464–4500.

35 L. M. Arellano, H. B. Habtom, Y. Jang, M. Barrejon, C. Parejo, J. C. Alvarez, M. J. Gomez-Escalonilla, A. Saste-Santos, F. D'Souza and F. Langa, Formation and photoinduced electron transfer in porphyrin- and phthalocyanine-bearing N-doped graphene hybrids synthesized by click chemistry, *Chem. – Eur. J.*, 2022, **28**, e2022200254.

36 J. R. Lakowicz, *Principles of fluorescence spectroscopy*, Springer, Singapore, 3rd edn, 2006, pp. 63–673.

37 C. B. KC and F. D'Souza, Design and photochemical study of supramolecular donor-acceptor systems assembled via metal-ligand axial coordination, *Coord. Chem. Rev.*, 2016, **322**, 104–141.

38 C. A. Wijeninghe, M. Niemi, N. V. Tkachenko, N. K. Subbaiyan, M. E. Zandler, H. Lemmetyinen and F. D'Souza, Photoinduced electron transfer in a directly linked meso-triphenylamine zinc porphyrin-quinone dyad, *J. Porphyr. Phthalocyanines*, 2011, **15**, 391–400.

39 F. D'Souza, Molecular recognition via hydroquinone-quinone pairing: electrochemical and singlet emission behavior of 5,0,15-triphenyl-20-(2,5-dihydroxyphenyl)porphyrinato zinc(II)-quinone complex, *J. Am. Chem. Soc.*, 1996, **118**, 923–924.

This journal is © The Royal Society of Chemistry 2022